Dominance of γ - γ electron-positron pair creation in a plasma driven by high-intensity lasers

Y. He,^{1,*} T. G. Blackburn,² T. Toncian,³ and A. V. Arefiev^{1,†}

¹University of California at San Diego, La Jolla, California 92093, USA
²Department of Physics, University of Gothenburg, SE-41296 Gothenburg, Sweden
³Institute for Radiation Physics, Helmholtz-Zentrum Dresden-Rossendorf e.V., 01328 Dresden, Germany
(Dated: June 1, 2022)

Creation of electrons and positrons from light alone is a basic prediction of quantum electrodynamics, but yet to be observed. Here we show that it is possible to create $>10^8$ positrons by dual laser irradiation of a structured plasma target, at intensities of 2×10^{22} Wcm⁻². In contrast to previous work, the pair creation is primarily driven by the linear Breit-Wheeler process $(\gamma\gamma\to e^+e^-)$, not the nonlinear process assumed to be dominant at high intensity, because of the high density of γ rays emitted inside the target. The favorable scaling with laser intensity of the linear process prompts reconsideration of its neglect in simulation studies, but also permits positron jet formation at intensities that are already experimentally feasible. Simulations show that the positrons, confined by a quasistatic plasma magnetic field, may be accelerated by the lasers to energies > 200 MeV.

High-power lasers, focused close to the diffraction limit, create ultrastrong electromagnetic fields that can be harnessed to drive high fluxes of energetic particles and to study fundamental physical phenomena [1]. At intensities exceeding 10²³ Wcm⁻², those energetic particles can drive nonlinear quantum-electrodynamical (QED) processes [2, 3] otherwise only found in extreme astrophysical environments [4, 5]. One such process is the creation of matter and antimatter, namely electron-positron pairs, from light alone. Whereas multiphoton (nonlinear) pair creation has been measured once, using an intense laser [6], the perturbative, two-photon process $(\gamma\gamma \to e^+e^-)$, referred to here as the linear Breit-Wheeler process [7]) has yet to be observed in the laboratory with real photons. The nonlinear process may be viewed as the 'decay' of a photon due to the presence of a strong electromagnetic field; as the probability grows nonperturbatively with increasing field strength [8, 9], it is expected to provide the dominant contribution to pair cascades in high-field environments, including laser-matter interactions beyond the current intensity frontier [10, 11] and pulsar magnetospheres [12].

The small size of the linear Breit-Wheeler cross section means that high photon flux is necessary for its observation. Achieving the necessary flux requires specialized experimental configurations [13, 14] and therefore its possible contribution to in situ electron-positron pair creation has hitherto been neglected in studies of high-intensity laser-matter interactions. However, lasermatter interactions create not only regions of ultrastrong electromagnetic field, but also high fluxes of accelerated particles, because relativistic effects mean that even a solid-density target can become transparent to intense laser light [15, 16]. In the situation of multiple colliding laser pulses, which is the most advantageous geometry for driving nonlinear QED cascades [10, 17–19], there are, as a consequence, dense, counterpropagating flashes of γ rays, and so the neglect of linear pair creation may

not be appropriate.

Here we show that, in the dual laser irradiation of a structured plasma target, the linear process is dominant over the nonlinear for intensities $I_0 < 5 \times 10^{22} \text{ Wcm}^{-2}$, at which the positron yield is $\sim 10^9$, four orders of magnitude greater than that envisaged in [13, 14]. These positrons are generated when two high-energy electron beams, accelerated by and copropagating with laser pulses that are guided along a plasma channel, collide head-on in a strong-field region, emitting synchrotron photons that collide with each other and the respective oncoming laser. Not only does this provide an opportunity to study the linear Breit-Wheeler process itself, which is of interest because of its role in astrophysics [20– 22, but also the transition between linear and nonlineardominated pair cascades. In an astrophysical context, the balance between these two determines how a pulsar magnetosphere is filled with plasma; as in the laser-plasma scenario, the controlling factors are the field strength and photon flux, which are affected by, e.g., the specific region of the magnetosphere and the age of the pulsar [23– 26]. We also show that the positrons, created inside the plasma channel coterminously with the laser pulses, may be confined and accelerated to energies of hundreds of MeV, which raises the possibility of generating positron jets.

The target configuration considered in this Letter is shown in Fig. 1(a). A structured plastic target with a pre-filled channel is irradiated from both sides by two 50-fs, high-intensity laser pulses that have the same peak normalized laser amplitude a_0 . Here $a_0 = 0.85 I_0^{1/2} [10^{18} \mathrm{W cm}^{-2}] \lambda_0 [\mu \mathrm{m}]$, where I_0 is the peak intensity of the laser and $\lambda_0 = 1$ $\mu \mathrm{m}$ its wavelength in vacuum. We investigate pair production in the range $100 \leq a_0 \leq 190$ or, equivalently, $1.4 \times 10^{22} \leq I_0 [\mathrm{W cm}^{-2}] \leq 4.9 \times 10^{22}$. The purpose of the target structure, where a channel of width $d_{\mathrm{ch}} = 5$ $\mu \mathrm{m}$ and electron density $n_{\varepsilon} = (a_0/100)3.8n_c$ is embedded in a bulk with higher

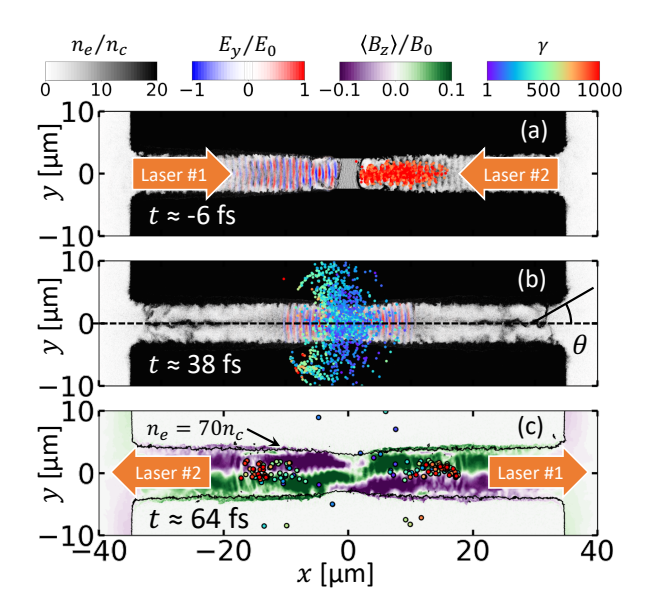


FIG. 1. Structured plasma target during irradiation by two laser pulses ($a_0=190$). (a) Electron density (gray scale), transverse electric field of laser #1 (color scale) and energetic electrons with $\gamma_e \geq 800$ accelerated by laser #2 (dots, colored by γ_e). (b) Total transverse electric field (color scale) and electrons from panel (a). (c) Laser-accelerated positrons (points), confined by the quasistatic plasma magnetic field $\langle B_z \rangle$ (color scale). E_0 and B_0 are the laser electric and magnetic fields in vacuum.

density $n_e = 100n_c$, is to achieve stable propagation [27] and alignment of the two lasers. (The classical cutoff, or critical, density $n_c = \pi mc^2/(e\lambda_0)^2$, where e is the elementary charge, m is the electron mass, and c is the speed of light.) The scaling of the channel density with a_0 ensures that the optical properties of the channel remain approximately the same with increase of a_0 . With regard to practical realization of this geometry, we note that structured targets with empty channels have successfully been used in experiments [28, 29] and that it is now possible to fabricate targets with prefilled channels, similar to those considered in this work [30]. The ion species is chosen to be fully ionized carbon, such that Bethe-Heitler pair creation, which has already been demonstrated in laser-driven experiments [31, 32], may be neglected. The interaction is simulated in 2D with the fully relativistic particle-in-cell (PIC) code EPOCH [33], which includes a Monte Carlo implementation of quantum synchrotron radiation and nonlinear pair creation [34]. Detailed simulation and target parameters are provided in the Supplemental Material. All the results presented in this Letter have been appropriately normalized by taking the size of the ignored dimension to be equal to the channel width $d_{\rm ch}$, i.e. 5 μ m.

The plasma channel, being relativistically transparent to the intense laser light [15, 16], acts as an optical waveguide. The laser pulses propagate with nearly constant transverse size through the channel, pushing plasma elec-

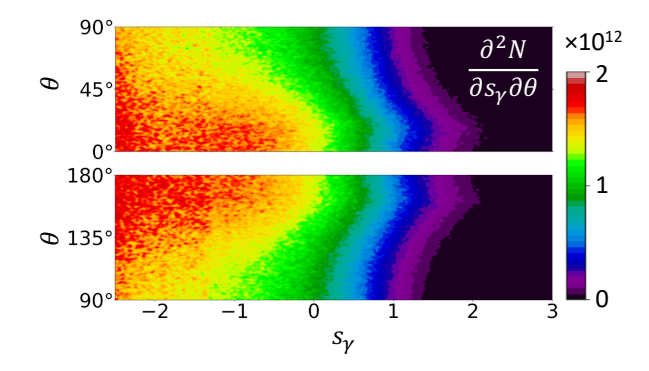


FIG. 2. Energy-angle spectrum, $\partial^2 N/(\partial s_\gamma \partial \theta)$ [°-1], of the photons emitted inside the channel, where θ is the angle defined in Fig. 1(b) and $s_\gamma \equiv \log_{10}(\epsilon_\gamma [\text{MeV}])$. The spectrum for $-180^\circ \leq \theta \leq 0^\circ$ is similar.

trons forward. This longitudinal current generates a slowly evolving, azimuthal magnetic field with peak magnitude 0.6 MT (30% of the laser magnetic field strength) at $a_0=190$. The magnetic field enables confinement and direct laser acceleration of the electrons [27, 35]. After propagating for $\sim 30~\mu m$ along the channel, laser #2 in Fig. 1(a) has accelerated a left-moving, high-energy, high-charge electron beam that performs transverse oscillations of amplitude $\sim 2~\mu m$: the number of electrons with energy greater than 400 MeV ($\gamma_e > 800$) is 4×10^{11} , which is equivalent to a charge of 64 nC. (Laser #1 generates a similar population of electrons moving to the right.)

The target length is such that no appreciable depletion of the laser pulses occurs by the time they reach the midplane (x = 0), t = 0. Here, the high-energy electron beams collide head-on with the respective oncoming laser pulse, each of which still has almost its full intensity. This configuration maximizes the quantum nonlinearity parameter $\chi_e \approx 0.5(1 \pm \cos \theta)(\gamma_e/1000)(a_0/200)\lambda_0^{-1}[\mu m],$ where θ is the angle between the particle velocity and the x-axis and the positive (negative) sign refers to electrons moving to the right (left). Figure 1(b) shows the impact of the collision on the energetic electrons from Fig. 1(a): they radiate away a substantial fraction of the energy they gained during the acceleration phase and are scattered out of the channel. The configuration under consideration here therefore represents a micron-scale, plasma-based realization of an all-optical laser-electronbeam collision (see also [17]). This geometry is the subject of theoretical [36–38] and experimental [39, 40] investigation into radiative energy loss in the quantum regime, as well as nonlinear pair creation [41].

The angularly resolved spectrum of the emitted photons is shown in Fig. 2. There are approximately 2×10^{14} photons with energies between 100 keV and 10 MeV and with $90^{\circ} \leq \theta \leq 180^{\circ}$. This is essentially half of the energetic photons emitted by the left-moving electrons (the other half is emitted with $-180^{\circ} \leq \theta \leq -90^{\circ}$ and

has a similar spectrum). The photons emitted by one electron beam collide with both the oncoming laser and the photons emitted by the other electron beam. The former drives electron-positron pair creation by the nonlinear Breit-Wheeler process, $\gamma \xrightarrow{\rm EM\ field} e^+e^-$ [2, 9]: at $a_0=190$, our simulations predict a yield of 5×10^8 pairs. The positrons subsequently undergo direct laser acceleration in much the way as the electrons: as it propagates from $x\approx 0$ to $x\approx 20~\mu{\rm m}$, the typical Lorentz factor of a right-moving positron increases to $\gamma_{e^+}\approx 1000$ [the latter shown in Fig. 1(c)].

Positron acceleration is made possible by the plasma magnetic field. The field induced by laser #2 on the right-hand-side of the target, during the electron acceleration phase, is confining for electrons moving to the left, or equivalently, positrons moving to the right. Crucially, Fig. 1(c) shows that this magnetic field topology is preserved well after the lasers and electron beams collide. As the laser pulses continue to propagate along the channel, this raises the possibility of generating high-energy positron jets, if the pair creation in the channel center is sufficiently prolific. We now show that this is the case, and furthermore that the pair creation is dominated by the linear Breit-Wheeler process.

Let us estimate the number of positrons created by the linear process, $N_{\rm lin}^{\rm BW}$. The cross section is [7]:

$$\sigma_{\gamma\gamma} = \frac{\pi r_e^2}{2\varsigma} \left[(3 - \beta^4) \ln \left(\frac{1+\beta}{1-\beta} \right) - 2\beta (2-\beta^2) \right], \quad (1)$$

where $r_e = e^2/(mc^2)$ is the classical electron radius, $\beta = \sqrt{1-1/\varsigma}$, and $\sqrt{\varsigma}$ is the normalized center-of-mass energy, $\varsigma = \epsilon_1 \epsilon_2 (1-\cos\psi)/(2m^2c^4)$, for two photons with energy $\epsilon_{1,2}$ colliding at angle ψ . Note that Eq. (1) is the cross section for two-photon pair creation in vacuum. While a strong EM field is known to modify the cross section [42–44], these corrections, which scale as $(\chi_{\gamma}/\varsigma)^2$ for photon quantum nonlinearity parameter χ_{γ} [45], are negligible for the scenario under consideration here (see the Supplemental Material for details).

We take as a representative value of the cross section $\sigma_{\gamma\gamma}\approx 2r_e^2$ (approximately its maximum, at $\varsigma\approx 2$) and assume that we have two photon populations of number density n_γ , colliding head-on in a volume of length $c\tau$ (the laser pulse length) and width $d_{\rm ch}$ (the width of the channel). The number of photons (in each beam) is $N_\gamma\approx 10^9\lambda_0[\mu{\rm m}]P_\gamma(n_e/n_c)(c\tau/\lambda_0)(d_{\rm ch}/\lambda_0)^2$ and the number of positrons produced is $N_{\rm lin}^{\rm BW}\approx 40P_\gamma^2(n_e/n_c)^2(c\tau/\lambda_0)^2(d_{\rm ch}/\lambda_0)^2$, where P_γ is the number of photons emitted per electron, n_e the electron number density and λ_0 the laser wavelength. The physical parameters are $n_e=7n_c$, $\tau=50$ fs, $d_{\rm ch}=5$ µm, and $\lambda_0=1$ µm. The number of photons emitted in a single laser period by a counterpropagating electron is $P_\gamma\approx 18\alpha a_0$. By setting $P_\gamma=20$, we obtain a total number of photons, $2N_\gamma\approx 1.3\times 10^{14}$, which is approximately consistent with

the simulation result. As a consequence, we predict that $N_{\rm lin}^{\rm BW} \approx 7 \times 10^9$. Moreover, given that $P_{\gamma} \propto a_0$ and $n_e \propto a_0$, we expect a scaling of $N_{\rm lin}^{\rm BW} \propto a_0^4$.

This is considerably larger than the number of pairs expected from the nonlinear Breit-Wheeler process; moreover, as the probability rate for the latter scales is exponentially suppressed with decreasing a_0 , we expect the yield to be much more sensitive to reductions in laser intensity. The potential dominance of the linear process motivates a precise computation, which takes into the account the energy, angle and temporal dependence of the photon emission.

However, direct implementation of the linear Breit-Wheeler process in a PIC code represents a significant computational challenge, as it involves binary collisions of macroparticles and the interaction must be simulated in at least 2D. The simulation at $a_0=190$ generates $\sim 10^8$ macrophotons in the energy range relevant for linear Breit-Wheeler pair creation and therefore $\sim 10^{16}$ possible pairings. The number of pairings that needs to be checked can be reduced by using bounding volume hierarchies [46], which is effective if the photon emission and the pair creation are well-separated in time and space. In our case, there is no such separation.

In order to compute the pair yield and spatial distribution, we approximate the photon population as a collection of collimated mono-energetic beamlets. Discretization into beamlets is achieved by recording the location (x_0, y_0) , energy ϵ_{γ} , and angle θ of each photon macroparticle at the time of the emission t_{emit} . The photon emission pattern suggests that the emission profile across the channel can be approximated as uniform. We thus represent the emitted photons by a timedependent distribution function $f = f(x_0, s_\gamma, \theta; t_{emit}),$ where $s_{\gamma} \equiv \log_{10}(\epsilon_{\gamma}/\text{MeV})$. It is sufficient to limit our analysis to $-40 \ \mu \text{m} \le x_0 \le 40 \ \mu \text{m}, -3 \le s_{\gamma} < 3$, and $0^{\circ} \le \theta \le 180^{\circ}$. We split each interval into 70 equal segments to obtain 2.6×10^5 beamlets that contain photons. Our simplification is to only check for the collisions of beamlets propagating to the right with beamlets propagating to the left. The yield is multiplied by a factor of two to account for beamlets with $-180^{\circ} \le \theta \le 0^{\circ}$.

A beamlet has temporal dependence represented by photon slices of variable density with the thickness set by the spatial discretization. For a given pair of beamlets, our algorithm finds the interaction volume V, the location where the axes of the beamlets intersect and the intersection angle ψ . The total pair yield by these beamlets is calculated according to $\Delta N_{lin}^{BW} = \sigma_{\gamma\gamma}c(1-\cos\psi)V\int n_1n_2dt$, where n_1 and n_2 are the photon densities in two slices overlapping at the intersection point. In general, the shape of the overlapping region is not rectangular, so in order to visualize the pair production we uniformly deposit ΔN_{lin}^{BW} onto a rectangular grid, into cells with centers inside volume V. The procedure is repeated for each beamlet pairing to obtain the density of

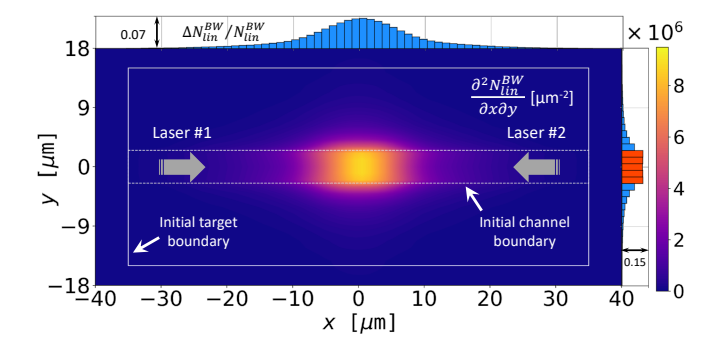


FIG. 3. (color scale) Probability density that an electronpositron pair is created by the linear Breit-Wheeler process at longitudinal and transverse coordinate x and y, when a structured target is irradiated by two laser pulses with peak normalized amplitude $a_0 = 190$. The density integrated over x(y), and normalized to the total number of pairs, is shown to the right (above).

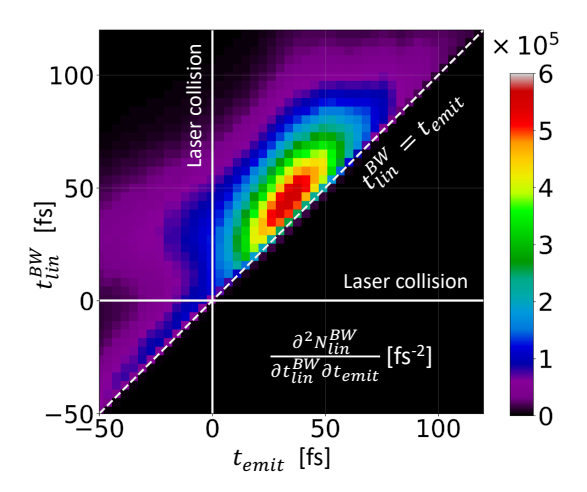


FIG. 4. (color scale) Probability density that an electron-positron pair is created by the linear Breit-Wheeler process at time $t_{\rm lin}^{\rm BW}$, by photons that were emitted at times $t_{\rm emit}$, when a structured target is irradiated by two laser pulses with peak normalized amplitude $a_0=190$. (The density includes a normalizing factor of 1/2 because each pair has two parent photons.)

generated pairs.

The algorithm is a simplification that replaces a direct approach of evaluating all possible collisions of beamlet slices. In a head-on collision, each slice collides with many counter-propagating slices within the interaction volume, which makes the calculation computationally intensive. Our algorithm takes advantage of the fact that the typical duration of beamlet emission, τ , is much longer than the time it takes for photons to travel between the sources emitting the two beamlets, l/c, where l is the distance between the sources in the case of near head-on collision. As shown in the Supplemental Material, our approach is a good approximation as long as $l/c\tau < 1$, with the error scaling as $(l/c\tau)^2$.

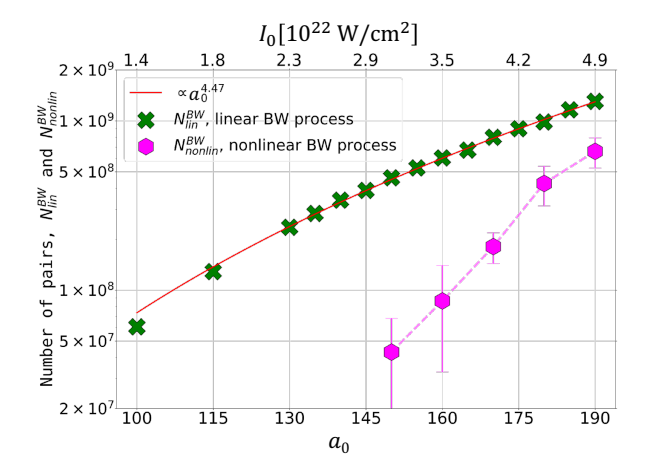


FIG. 5. The number of electron-positron pairs created by the linear and nonlinear Breit-Wheeler processes (green crosses and magenta points, respectively), for the setup shown in Fig. 1, at given laser amplitude a_0 (and equivalent peak intensity I_0). Error bars on the nonlinear results indicate statistical uncertainties: see text for details.

The location and time that pairs are created by the linear process, as determined by this algorithm for the case that $a_0 = 190$, are shown in Fig. 3 and Fig. 4 respectively. Approximately 59% of the pairs are created inside the original channel boundary, which is indicated by the white, dashed line in Fig. 3. The majority of the photons that drive the linear pair creation are emitted after the lasers collide, i.e. when the high-energy electrons are accelerated by the fields of the respective counterpropagating laser. Figure 4 shows the distribution of the electron-positron pairs in terms of their creation time, $t_{\rm lin}^{\rm BW}$, and the emission times of their parent photons, $t_{\rm emit}$. The distribution is scaled by a factor of 1/2 as each pair has two parent photons and therefore two relevant values of $t_{\rm emit}$. The majority (74%) of pairs are created by photons emitted after t=0. There is a smaller contribution from photons that are emitted during the acceleration phase, $t_{\rm emit} < 0$, before the collision; radiation in this case is driven by the plasma magnetic field, because the energetic electrons are moving in the same direction as the laser [27, 47]. The dominance of the post-collision contribution is caused by the increase in the quantum parameter χ_e for counterpropagation. The fact the pair creation overlaps with the laser pulses (in both time and space) indicates that the positrons could be accelerated out of the channel, as the magnetic field, shown in Fig. 1(c), has the correct orientation to confine them.

The numbers of pairs created via the linear and nonlinear Breit-Wheeler processes are compared for varying peak normalized laser amplitude a_0 in Fig. 5. The results for the nonlinear process are obtained by performing four simulation runs for each value of a_0 with different random seeds: points and error bars give the mean and standard deviation obtained, respectively. At $a_0 < 145$, fewer than ten macropositrons are generated per run, so the corresponding data points are not shown. Our analytical estimates for linear Breit-Wheeler pair creation lead us to expect a yield that scales as a_0^4 : this is consistent with a power-law fit to the data in Fig. 5, which gives a scaling $\propto a_0^m$, where $m \approx 4.5 \pm 0.1$. Across the full range of intensities explored, we find that the linear pair yield is significantly larger than the nonlinear yield.

In conclusion, we demonstrate that laser-plasma interactions provide a platform to generate and accelerate positrons, created entirely by light and light, at intensities that are well within the reach of current high-power laser facilities. While previous research into pair creation at high intensity has focused largely on the nonlinear Breit-Wheeler process, we show that the high density of photons afforded by a laser-plasma interaction makes the linear process dominant instead. We note that while field-driven modifications to the cross section are rather weak in the present scenario, our results motivate a more general treatment that can investigate where these corrections become substantial. The theory for a related process, pair annihiliation to two photons in a pulsed, plane EM wave, has recently been revisited [48].

This research was supported by AFOSR (Grant No. FA9550-17-1-0382). Simulations were performed with EPOCH (developed under UK EPSRC Grants EP/G054950/1, EP/G056803/1, EP/G055165/1 and EP/ M022463/1) using high performance computing resources provided by TACC.

- * yuh087@eng.ucsd.edu † aarefiev@eng.ucsd.edu
- P. Zhang, S. S. Bulanov, D. Seipt, A. V. Arefiev, and A. G. R. Thomas, Relativistic plasma physics in supercritical fields, Phys. Plasmas 27, 050601 (2020).
- [2] T. Erber, High-energy electromagnetic conversion processes in intense magnetic fields, Rev. Mod. Phys. 38, 626 (1966).
- [3] A. Di Piazza, C. Müller, K. Z. Hatsagortsyan, and C. H. Keitel, Extremely high-intensity laser interactions with fundamental quantum systems, Rev. Mod. Phys. 84, 1177 (2012).
- [4] A. K. Harding and D. Lai, Physics of strongly magnetized neutron stars, Rep. Prog. Phys. 69, 2631 (2006).
- [5] R. Ruffini, G. Vereshchagin, and S.-S. Xue, Electron–positron pairs in physics and astrophysics: From heavy nuclei to black holes, Phys. Rep. 487, 1 (2010).
- [6] D. L. Burke, R. C. Field, G. Horton-Smith, J. E. Spencer, D. Walz, S. C. Berridge, W. M. Bugg, K. Shmakov, A. W. Weidemann, C. Bula, K. T. McDonald, E. J. Prebys, C. Bamber, S. J. Boege, T. Koffas, T. Kotseroglou, A. C. Melissinos, D. D. Meyerhofer, D. A. Reis, and W. Ragg, Positron production in multiphoton light-by-light scattering, Phys. Rev. Lett. 79, 1626 (1997).
- [7] G. Breit and J. A. Wheeler, Collision of two light quanta,

- Phys. Rev. 46, 1087 (1934).
- [8] H. R. Reiss, Absorption of light by light, J. Math. Phys. 3, 59 (1962).
- [9] V. I. Ritus, Quantum effects of the interaction of elementary particles with an intense electromagnetic field, J. Sov. Laser Res. 6, 497 (1985).
- [10] A. R. Bell and J. G. Kirk, Possibility of prolific pair production with high-power lasers, Phys. Rev. Lett. 101, 200403 (2008).
- [11] C. P. Ridgers, C. S. Brady, R. Duclous, J. G. Kirk, K. Bennett, T. D. Arber, A. P. L. Robinson, and A. R. Bell, Dense electron-positron plasmas and ultraintense γ rays from laser-irradiated solids, Phys. Rev. Lett. **108**, 165006 (2012).
- [12] A. N. Timokhin and A. K. Harding, On the maximum pair multiplicity of pulsar cascades, Astrophys. J. 871, 12 (2019).
- [13] O. Pike, F. Mackenroth, H. E. G., and S. J. Rose, A photon-photon collider in a vacuum hohlraum, Nat. Photon. 8, 434 (2014).
- [14] X. Ribeyre, E. d'Humières, O. Jansen, S. Jequier, V. T. Tikhonchuk, and M. Lobet, Pair creation in collision of γ-ray beams produced with high-intensity lasers, Phys. Rev. E 93, 013201 (2016).
- [15] P. Kaw and J. Dawson, Relativistic nonlinear propagation of laser beams in cold overdense plasmas, Phys. Fluids 13, 472 (1970).
- [16] S. Palaniyappan, B. M. Hegelich, H.-C. Wu, D. Jung, D. C. Gautier, L. Yin, B. J. Albright, R. P. Johnson, T. Shimada, S. Letzring, D. T. Offermann, J. Ren, C. Huang, R. Hörlein, B. Dromey, J. C. Fernandez, and R. C. Shah, Dynamics of relativistic transparency and optical shuttering in expanding overdense plasmas, Nat. Phys. 8, 763 (2012).
- [17] X.-L. Zhu, T.-P. Yu, Z.-M. Sheng, Y. Yin, I. C. E. Turcu, and A. Pukhov, Dense GeV electron-positron pairs generated by lasers in near-critical-density plasmas, Nat. Commun. 7, 13686 (2016).
- [18] T. Grismayer, M. Vranic, J. L. Martins, R. A. Fonseca, and L. O. Silva, Seeded QED cascades in counterpropagating laser pulses, Phys. Rev. E 95, 023210 (2017).
- [19] A. Gonoskov, A. Bashinov, S. Bastrakov, E. Efimenko, A. Ilderton, A. Kim, M. Marklund, I. Meyerov, A. Muraviev, and A. Sergeev, Ultrabright GeV photon source via controlled electromagnetic cascades in laser-dipole waves, Phys. Rev. X 7, 041003 (2017).
- [20] R. J. Gould and G. Schréder, Opacity of the universe to high-energy photons, Phys. Rev. Lett. 16, 252 (1966).
- [21] S. Bonometto and M. J. Rees, On possible observable effects of electron pair production in QSOs, Mon. Not. R. Astron. Soc. 152, 21 (1971).
- [22] T. Piran, The physics of gamma-ray bursts, Rev. Mod. Phys. 76, 1143 (2005).
- [23] M. L. Burns and A. K. Harding, Pair production rates in mildly relativistic magnetized plasmas, Astrophys. J. 285, 747 (1984).
- [24] B. Zhang and G. J. Qiao, Two-photon annihilation in the pair formation cascades in pulsar polar caps, Astron. Astrophys. 338, 62 (1998).
- [25] G. Voisin, F. Mottez, and S. Bonazzola, Electronpositron pair production by gamma-rays in an anisotropic flux of soft photons, and application to pulsar polar caps, Mon. Not. R. Astron. Soc. 474, 1436 (2017).
- [26] A. Y. Chen, F. Cruz, and A. Spitkovsky, Filling the

- magnetospheres of weak pulsars, Astrophys. J. 889, 69 (2020).
- [27] D. J. Stark, T. Toncian, and A. V. Arefiev, Enhanced multi-MeV photon emission by a laser-driven electron beam in a self-generated magnetic field, Phys. Rev. Lett. 116, 185003 (2016).
- [28] J. Snyder, L. L. Ji, K. M. George, C. Willis, G. E. Cochran, R. L. Daskalova, A. Handler, T. Rubin, P. L. Poole, D. Nasir, A. Zingale, E. Chowdhury, B. F. Shen, and D. W. Schumacher, Relativistic laser driven electron accelerator using micro-channel plasma targets, Phys. Plasmas 26, 033110 (2019).
- [29] M. Bailly-Grandvaux, D. Kawahito, C. McGuffey, J. Strehlow, B. Edghill, M. S. Wei, N. Alexander, A. Haid, C. Brabetz, V. Bagnoud, R. Hollinger, M. G. Capeluto, J. J. Rocca, and F. N. Beg, Ion acceleration from microstructured targets irradiated by high-intensity picosecond laser pulses, Phys. Rev. E 102, 021201 (2020).
- [30] J. Williams, Private communications at General Atomics, 2019.
- [31] H. Chen, S. C. Wilks, J. D. Bonlie, E. P. Liang, J. Myatt, D. F. Price, D. D. Meyerhofer, and P. Beiersdorfer, Relativistic positron creation using ultraintense short pulse lasers, Phys. Rev. Lett. 102, 105001 (2009).
- [32] G. Sarri, W. Schumaker, A. Di Piazza, M. Vargas, B. Dromey, M. E. Dieckmann, V. Chvykov, A. Maksimchuk, V. Yanovsky, Z. H. He, B. X. Hou, J. A. Nees, A. G. R. Thomas, C. H. Keitel, M. Zepf, and K. Krushelnick, Table-top laser-based source of femtosecond, collimated, ultrarelativistic positron beams, Phys. Rev. Lett. 110, 255002 (2013).
- [33] T. D. Arber, K. Bennett, C. S. Brady, A. Lawrence-Douglas, M. G. Ramsay, N. J. Sircombe, P. Gillies, R. G. Evans, H. Schmitz, A. R. Bell, and C. P. Ridgers, Contemporary particle-in-cell approach to laser-plasma modelling, Plasma Phys. Control. Fusion 57, 113001 (2015).
- [34] C. P. Ridgers, J. G. Kirk, R. Duclous, T. G. Blackburn, C. S. Brady, K. Bennett, T. D. Arber, and A. R. Bell, Modelling gamma-ray photon emission and pair production in high-intensity laser-matter interactions, J. Comp. Phys. 260, 273 (2014).
- [35] Z. Gong, F. Mackenroth, T. Wang, X. Q. Yan, T. Toncian, and A. V. Arefiev, Direct laser acceleration of electrons assisted by strong laser-driven azimuthal plasma magnetic fields, Phys. Rev. E 102, 013206 (2020).
- [36] N. Neitz and A. Di Piazza, Stochasticity effects in quantum radiation reaction, Phys. Rev. Lett. 111, 054802 (2013).
- [37] T. G. Blackburn, C. P. Ridgers, J. G. Kirk, and A. R. Bell, Quantum radiation reaction in laser–electron-beam collisions, Phys. Rev. Lett. 112, 015001 (2014).
- [38] M. Vranic, T. Grismayer, R. A. Fonseca, and L. O. Silva,

- Quantum radiation reaction in head-on laser-electron beam interaction, New J. Phys. 18, 073035 (2016).
- [39] J. M. Cole, K. T. Behm, E. Gerstmayr, T. G. Blackburn, J. C. Wood, C. D. Baird, M. J. Duff, C. Harvey, A. Ilderton, A. S. Joglekar, K. Krushelnick, S. Kuschel, M. Marklund, P. McKenna, C. D. Murphy, K. Poder, C. P. Ridgers, G. M. Samarin, G. Sarri, D. R. Symes, A. G. R. Thomas, J. Warwick, M. Zepf, Z. Najmudin, and S. P. D. Mangles, Experimental evidence of radiation reaction in the collision of a high-intensity laser pulse with a laser-wakefield accelerated electron beam, Phys. Rev. X 8, 011020 (2018).
- [40] K. Poder, M. Tamburini, G. Sarri, A. Di Piazza, S. Kuschel, C. D. Baird, K. Behm, S. Bohlen, J. M. Cole, D. J. Corvan, M. Duff, E. Gerstmayr, C. H. Keitel, K. Krushelnick, S. P. D. Mangles, P. McKenna, C. D. Murphy, Z. Najmudin, C. P. Ridgers, G. M. Samarin, D. R. Symes, A. G. R. Thomas, J. Warwick, and M. Zepf, Experimental signatures of the quantum nature of radiation reaction in the field of an ultraintense laser, Phys. Rev. X 8, 031004 (2018).
- [41] M. Lobet, X. Davoine, E. d'Humières, and L. Gremillet, Generation of high-energy electron-positron pairs in the collision of a laser-accelerated electron beam with a multipetawatt laser, Phys. Rev. Accel. Beams 20, 043401 (2017).
- [42] Y. J. Ng and W. Tsai, Pair creation by photon-photon scattering in a strong magnetic field, Phys. Rev. D 16, 286 (1977).
- [43] A. A. Kozlenkov and I. G. Mitrofanov, Two-photon production of e^{\pm} pairs in a strong magnetic field, Sov. Phys. JETP **64**, 1173 (1986).
- [44] A. Hartin, Strong field QED in lepton colliders and electron/laser interactions, Int. J. Mod. Phys. A 33, 1830011 (2018); Second Order QED Processes in an Intense Electromagnetic Field, Ph.D. thesis, University of London (2006).
- [45] V. N. Baier, V. M. Katkov, and V. M. Strakhovenko, Electromagnetic Processes at High Energies in Oriented Single Crystals (World Scientific, Singapore, 1998).
- [46] O. Jansen, E. d'Humières, X. Ribeyre, S. Jequier, and V. T. Tikhonchuk, Tree code for collision detection of large numbers of particles applied to the Breit-Wheeler process, J. Comp. Phys. 355, 582 (2018).
- [47] T. Wang, X. Ribeyre, Z. Gong, O. Jansen, E. d'Humières, D. Stutman, T. Toncian, and A. Arefiev, Power scaling for collimated γ-ray beams generated by structured laserirradiated targets and its application to two-photon pair production, Phys. Rev. Applied 13, 054024 (2020).
- [48] S. Bragin and A. D. Piazza, Electron-positron annihilation into two photons in an intense plane-wave field (2020), arXiv:2003.02231 [hep-ph].

Supplemental Material:

Dominance of γ - γ electron-positron pair creation in a plasma driven by high-intensity lasers

Y. He,¹ T. G. Blackburn,² T. Toncian,³ and A. V. Arefiev¹

¹University of California at San Diego, La Jolla, California 92093, USA
²Department of Physics, University of Gothenburg, SE-41296 Gothenburg, Sweden
³Institute for Radiation Physics, Helmholtz-Zentrum Dresden-Rossendorf e.V., 01328 Dresden, Germany
(Dated: June 1, 2022)

2D PIC SIMULATION SETUP

Table I provides detailed parameters for the simulations presented in the Letter. Simulations were carried out using the fully relativistic particle-in-cell code EPOCH [1]. All our simulations are 2D-3V.

The axis of the structured target is aligned with the axis of the counter-propagating lasers (laser #1 and laser #2) at y=0. The target is initialized as a fully-ionized plasma with carbon ions. The bulk electron density is constant during the intensity scan while the electron density in the channel is set at $n_e=(a_0/100)3.8n_c$. Each laser is focused at the corresponding channel opening. The lasers are linearly polarized with the electric field being in the plane of the simulation. In the absence of the target, the lasers have the same Gaussian profile in the focal spot with the same Gaussian temporal profile.

We performed additional runs at $a_0 = 190$ with lower and higher spatial resolutions (40 by 20 cells per μ m and 80 by 80 cells per μ m). There are no significant variations in the photon spectra for multi-MeV photons and for photons with energies above 50 keV.

DISTRIBUTION OF LINEAR BREIT-WHEELER PAIRS

In the Letter, we only consider photons in the energy given by the condition $-3 \le s_{\gamma} < 3$, where $s_{\gamma} = \log_{10}(\epsilon_{\gamma}/\text{MeV})$ and ϵ_{γ} is the photon energy. To show that this approach is justified, we have plotted the distribution of linear Breit-Wheeler pairs as a function of photon energies. We use s_{γ} rather than ϵ_{γ} to capture a wide range of energies. Figure 1 confirms that the pair yield drops off for $|s_{\gamma}| > 2$, which justifies the energy range selected in the Letter.

DISTRIBUTION OF NONLINEAR BREIT-WHEELER PAIRS

Figure 2 provides additional information on the production of nonlinear Breit-Wheeler pairs. The horizontal scale shows the emission time, t_{emit} , of energetic photons that collide with the lower energy photons to produce pairs. The energetic photons are generated and subsequently propagated as particles by the PIC code. The time of the pair production, t_{nonlin}^{BW} , is shown along the vertical scale. The number of pairs for each pairing of t_{emit} and t_{nonlin}^{BW} is color-coded. The pair production is directly computed by the PIC code. The numbers shown in

Laser parameters		
Normalized field amplitude	$a_0 = 100 - 190$	
Peak intensity range	$I_0 = 1.4 - 4.9 \times 10^{22} \text{ W/cm}^2$	
Wavelength	$\lambda_0 = 1 \ \mu \text{m}$	
Focal plane of laser #1	$x = -35 \; \mu \text{m}$	
Focal plane of laser #2	$x = +35 \mu m$	
Laser profile (longitudinal and	Gaussian	
transverse)		
Pulse duration (FWHM for	50 fs	
intensity)		
Focal spot size (FWHM for	3.6 μm	
intensity)		

Target parameters	
Target thickness (along y)	30 μm
Target length (along x)	70 μm
Channel width	$d_{\rm ch} = 5 \ \mu \rm m$
Composition	C ⁺⁶ and electrons
Channel density	$n_e = 3.8 - 7.1 n_c$
Bulk density	$n_e = 100n_C$

Other parameters	
Simulation box	80 μm in x; 36 μm in y
Spatial resolution	40 cells per μm in x
	40 cells per μm in y
Macro-particles per cell	40 for electrons
	20 for carbon ions

TABLE I. 2D PIC simulation parameters.

the figure are obtained by assuming that the spatial scale along the z axis is equal to the initial width of the channel.

The vast majority of the nonlinear pairs are produced by photons emitted after the two lasers collide. Indeed, $t_{emit} = 0$ is the time when the two laser beams begin to collide. Most of the pairs are located at $t_{emit} > 0$, which indicates that the parent photons were generated after the collision.

STRONG-FIELD MODIFICATIONS TO THE LINEAR BREIT-WHEELER CROSS SECTION

The cross section we use to determine the number of electron-positron pairs created by the linear Breit-Wheeler process, Eq. (1), is calculated assuming that the photons are in vacuum. However, our calculations show that the pairs are created within the plasma channel as the laser pulses overlap, where the background electromagnetic field is strong. The

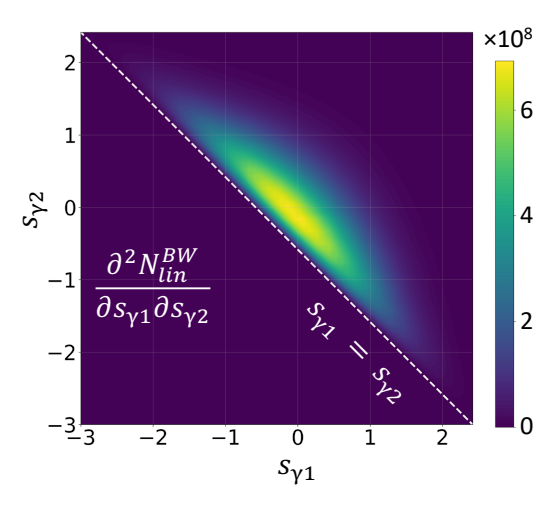


FIG. 1. Distribution of linear Breit-Wheeler pairs as a function of photon energies for colliding laser pulses with $a_0 = 190$.

presence of a strong magnetic field [2, 3] or plane EM wave is known to modify the cross section for this process. Calculations of the cross section in the latter case have focused on changes at moderate a_0 [4] or on resonance features [5]. Resonances occur where the intermediate fermion is on mass shell, which corresponds to the incoherent combination of nonlinear pair creation, followed by photon absorption by one of the daughter fermions, in the high-intensity regime. This contribution, which is effectively driven by a single photon, is already counted as our simulations include nonlinear pair creation; photon absorption by an electron in a strong field [6, 7] is suppressed unless the photon and electron are aligned within electron's emission cone. (See supporting simulations in [8].)

As such, in order to estimate the effect of the strong field at $a_0 \gg 1$, we use the cross section for two-photon pair creation in a constant, crossed field given in Sec. 5.7 of [9]. If two-photon pair creation is kinematically allowed, i.e. $\varsigma > 1$, corrections to the cross section scale as $(\chi_\gamma/\varsigma)^2$, where χ_γ is the quantum nonlinearity parameter [9]: in the scenario under consideration here, the photons which undergo linear pair creation have MeV energies and $\chi_\gamma \ll 1$, and therefore these corrections can be neglected. On the other hand, the fact the laser-plasma interactions provide a platform for prolific two-photon pair creation in a region of strong EM field, as our results show, motivates a more general treatment that can investigate where these field-driven corrections become substantial. We note that that a related process, pair annihiliation to two photons in a pulsed, plane EM wave, has recently been revisited [10].

PAIR PRODUCTION ALGORITHM FOR HEAD-ON COLLISIONS OF BEAMLETS

Our algorithm for computing the pair production yield due to the linear Breit-Wheeler process leverages the fact that the colliding photons are emitted over an extended period of time compared to the characteristic travel time between the emission

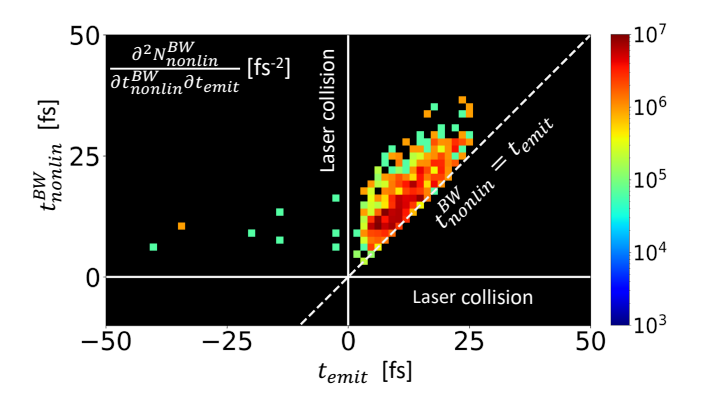


FIG. 2. Distribution function $\partial^2 N_{nonlin}^{BW}/(\partial t_{nonlin}^{BW}\partial t_{emit})$ [fs⁻²] on the number of electron-positron pairs over the time t_{nonlin}^{BW} of pair creation and the t_{emit} of parenting photons. The peak amplitude of each laser peak is $a_0=190$.

locations. In what follows, we illustrate its implementation for head-on collisions of two beamlets. Near head-on collisions are the biggest contributor to the pair yield and this is also the regime that greatly benefits from our simplified approach in terms of computational efficiency.

We are considering a head-on collision of two counterpropagating beamlets, as defined in the Letter, that have the same transverse area S. The first beamlet is being emitted at $x = x_1$ and it propagates in the positive direction. It is convenient to use the emission time τ as a marker for the photons in each beamlet. The corresponding photon density in the first beamlet is then $n_1(\tau_1)$. The counter-propagating beamlet is emitted at $x = x_2 > x_1$ and its photon density is $n_2(\tau_2)$. The total pair yield by these two beamlets interacting with each other is

$$\Delta N_{pairs} = \sigma_{\gamma\gamma} Sc^2 \int_{-\infty}^{+\infty} d\tau_1 n_1(\tau_1) \left[\int_{\tau_1 - l/c}^{\tau_1 + l/c} d\tau_2 n_2(\tau_2) \right], \tag{1}$$

where

$$l \equiv x_2 - x_1. \tag{2}$$

Equation (1) presents a direct approach to calculating the pair yield and it involves a double integral.

In our case, the typical beamlet emission lasts longer than l/c, which suggests a possible simplification of replacing $n_2(\tau_2)$ with $n_2(\tau_1)$. The inner integral in Eq. (1) can then be directly evaluated and we find that

$$\Delta N_{pairs} \approx 2c\sigma_{\gamma\gamma}V \int_{-\infty}^{+\infty} n_1(\tau)n_2(\tau)d\tau,$$
 (3)

where $V \equiv lS$ is the interaction volume. Note that the two beamlets are interchangeable in this expression. In order to estimate the error, we expand $n_2(\tau_2)$ around $\tau_2 = \tau_1$ and retain linear and quadratic terms in the expansion. The time integral of the linear term in Eq. (1) is equal to zero, which means that the error in our approach is determined by the quadratic term.

We thus estimate that the relative error in the number of produced pairs scales as $(l/c\Delta\tau)^2$, where $\Delta\tau$ is the characteristic duration of beamlet emission.

We compute the spatial distribution of pairs by simply assigning the pair density

$$\Delta n_{pairs} = \Delta N_{pairs} / V \tag{4}$$

to each position within the interaction volume. We call this the *average density method*. A direct approach would however require us to compute the following integral at each position along the *x* axis:

$$\Delta n_{pairs}^{direct}(x) = 2c\sigma_{\gamma\gamma} \int_{-\infty}^{+\infty} n_1(t_1) n_2(t_2) dt, \qquad (5)$$

where

$$t_1 = t - (x - x_1)/c,$$
 (6)

$$t_2 = t - (x_2 - x)/c.$$
 (7)

The direct approach is much more demanding computationally.

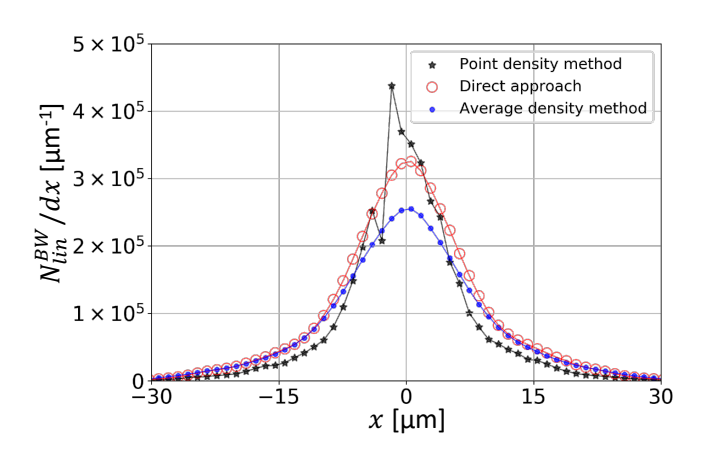


FIG. 3. Spatial distribution of linear Breit-Wheeler pairs produced in a head-on collision of spatially distributed beamlets. The three curves represent three different approaches: direct approach (open circles), average density method (solid circles), and point density method (star markers).

Even though our approach for calculating the spatial distribution of pairs is deliberately crude for a single pair of beamlets, it is effective when applied to a large ensemble of spatially distributed beamlets. As an example, we have carried out calculations for approximately 3000 spatially distributed beamlets, where 1573 beamlets are directed to the right and 1590 beamlets are directed to the left. The photon energy range is 0.19 MeV $< \epsilon_{\gamma} < 2.05$ MeV. We used our PIC simulation to generate these beamlets by selecting photons emitted with $|\theta| < 5.15^{\circ}$ or $|\theta - \pi| < 5.15^{\circ}$. The average density method

that uses Δn_{pairs} from Eq. (4) for each beamlet-beamlet collision gives the curve shown with small solid circles. The direct approach detailed by Eq. (5) gives the curve shown with open circles. The two curves have a similar shape, but the direct approach took almost two orders of magnitude longer in terms of computational time. The relative difference in the total number of pairs between the two methods is less than 17%.

Our method evenly distributes the generated pairs over the interaction volume, which is the key to achieving a good agreement with the direct but more computationally expensive approach. In order to illustrate this aspect, we performed another calculation. In this case, all of the pairs produced by two beamlets are placed into the center of the interaction volume without being evenly distributed. We call this the *point density method*. The density is calculated as $\Delta N_{pairs}/S\Delta x$, where ΔN_{pairs} is given by Eq. (3) and Δx is the thickness of slices that we use for spatial discretization into beamlets. The result of this procedure is shown with star markers in Fig. 3. There are no significant savings in terms of computational costs compared to the average density method. The characteristic width of the spatial distribution shows considerable deviation from that for the direct approach.

- [1] T. D. Arber, K. Bennett, C. S. Brady, A. Lawrence-Douglas, M. G. Ramsay, N. J. Sircombe, P. Gillies, R. G. Evans, H. Schmitz, A. R. Bell, and C. P. Ridgers, "Contemporary particle-in-cell approach to laser-plasma modelling," Plasma Phys. Control. Fusion 57, 113001 (2015).
- [2] Y. J. Ng and W. Tsai, "Pair creation by photon-photon scattering in a strong magnetic field," Phys. Rev. D 16, 286–294 (1977).
- [3] A. A. Kozlenkov and I. G. Mitrofanov, "Two-photon production of e[±] pairs in a strong magnetic field," Sov. Phys. JETP 64, 1173–1179 (1986).
- [4] O. I. Denisenko, "The Breit-Wheeler process in the laser field," Laser Phys. 18, 920–924 (2008).
- [5] A. Hartin, "Strong field QED in lepton colliders and electron/laser interactions," Int. J. Mod. Phys. A 33, 1830011 (2018); Second Order QED Processes in an Intense Electromagnetic Field, Ph.D. thesis, University of London (2006).
- [6] V. I. Ritus, "Quantum effects of the interaction of elementary particles with an intense electromagnetic field," J. Sov. Laser Res. 6, 497–617 (1985).
- [7] A. Ilderton, B. King, and A. J. MacLeod, "Absorption cross section in an intense plane wave background," Phys. Rev. D 100, 076002 (2019).
- [8] T. G. Blackburn, A. J. MacLeod, A. Ilderton, B. King, S. Tang, and M. Marklund, "Self-absorption of synchrotron radiation in a laser-irradiated plasma," (2020), arXiv:2005.00302 [physics.plasm-ph].
- [9] V. N. Baier, V. M. Katkov, and V. M. Strakhovenko, Electromagnetic Processes at High Energies in Oriented Single Crystals (World Scientific, Singapore, 1998).
- [10] S. Bragin and A. Di Piazza, "Electron-positron annihilation into two photons in an intense plane-wave field," (2020), arXiv:2003.02231 [hep-ph].